Information Sciences 430–431 (2018) 467–486

Contents lists available at ScienceDirect

Information Sciences

journal homepage: www.elsevier.com/locate/ins

A diversity indicator based on reference vectors for many-objective optimization

Xinye Cai [a,b,*], Haoran Sun [a,b], Zhun Fan [c]

[a] The College of Computer Science and Technology, Nanjing University of Aeronautics and Astronautics, Nanjing, Jiangsu 210016, PR China
[b] Collaborative Innovation Center of Novel Software Technology and Industrialization, Nanjing, Jiangsu 210016, PR China
[c] The Department of Electronic Engineering, School of Engineering, Shantou University, Guangdong, PR China

ARTICLE INFO

Article history:
Received 22 February 2017
Revised 20 November 2017
Accepted 26 November 2017
Available online 5 December 2017

Keywords:
Many-objective optimization
Diversity indicator
Online indicator
Offline indicator
Reference vector

ABSTRACT

Diversity estimation of Pareto front (PF) approximations is a critical issue in the field of evolutionary multiobjective optimization. However, the existing diversity indicators are usually inappropriate for PF approximations with more than three objectives. Many of them can be utilized only when compared with approximations obtained by multiple multiobjective optimizers, which makes them difficult to use online. In this paper, we propose a unary diversity indicator based on reference vectors (DIR) to estimate the diversity of PF approximations for many-objective optimization. In DIR, a set of uniform and widespread reference vectors are generated. The coverage of each solution in the objective space is evaluated by the number of representative reference vectors it is associated with. The diversity (both spread and uniformity) is determined by the standard deviation of the coverage for all the solutions. The smaller value of DIR, the better the diversity of a PF approximation is. DIR can be applied to a unary approximation without any compared approximations needed. Thus, DIR is easy to use as either an offline indicator to estimate the performance of an optimizer or an online indicator for the selection of solutions in a MOEA. In the experimental studies, both the artificial and the real PF approximations generated by seven different many-objective algorithms are used to verify DIR as an offline indicator. The effects of the number of reference vectors on DIR are also investigated. In addition, as an online indicator, DIR is integrated into a Pareto-dominance-based evolutionary multiobjective optimizer, NSGA-II. The experimental studies show it has the significant performance enhancements over the original NSGA-II on many-objective optimization problems.

1. Introduction

A multiobjective optimization problem (MOP) can be defined as follows:

$$\begin{aligned} &\text{minimize } F(x) = (f_1(x), \ldots, f_m(x))^T \\ &\text{subject to } x \in \Omega \end{aligned} \tag{1}$$

* Corresponding author at: Nanjing University of Aeronautics and Astronautics, College of Computer Science and Technology, Nanjing, Jiangsu 210016, PR China .

E-mail addresses: xinye@nuaa.edu.cn (X. Cai), zfan@stu.edu.cn (Z. Fan).

https://doi.org/10.1016/j.ins.2017.11.051
0020-0255/

where Ω is the *decision space*, F: $\Omega \to R^m$ consists of m real-valued objective functions. The *attainable objective set* is $\{F(x)|x \in \Omega\}$. Let u, $v \in R^m$, u is said to *dominate* v, denoted by $u \prec v$, if and only if $u_i \leq v_i$ for every $i \in \{1, \ldots, m\}$ and $u_j < v_j$ for at least one index $j \in \{1, \ldots, m\}$.[1] A solution $x^* \in \Omega$ is *Pareto-optimal* to (1) if there exists no solution $x \in \Omega$ such that $F(x)$ dominates $F(x^*)$. The set of all the Pareto-optimal points is called the *Pareto set* (*PS*) and the set of all the Pareto-optimal objective vectors is the *Pareto front* (*PF*) [37]. A PF approximation apparently can be very helpful for decision makers to understand the tradeoff relationship among different objectives and choose their preferred solutions. Over the past decades, multiobjective evolutionary algorithms (MOEAs) have been recognized as a major methodology for approximating the PFs in MOPs [9,15].

With the rapid growth of MOEAs [7,8,16,45] and other multiobjective optimizers [29] in the field of multiobjective optimization, the issue of performance assessment has become increasingly important. Various quality indicators [39,44,47] have already been proposed for performance evaluation. These indicators focus on one or several of the following aspects: 1) the convergence of the obtained PF approximation, 2) the spread (i.e., extensity) of the approximation and 3) the uniformity of the approximation. The latter two are closely related. Their combination is usually called the diversity of the approximation [32,39].

Many-objective optimization problems (MaOPs), i.e., MOPs with more than three objectives, appear widely in industrial and engineering design [18,24]. Over the recent years, the increasing amount of attention has been given to many-objective optimization in the community of MOEAs; and a wide variety of many-objective optimizers [10,13,33,43,48] have been developed and verified on problems with different characteristics [17,21,23].

However, the quality indicators to evaluate the performance of many-objective optimizers have not yet gained enough attention and concern [25]. Most indicators are infeasible or improper to evaluate PF approximations with a large number of objectives. In general, the difficulties of comparing multiple PF approximations may be summarized in the following reasons.

1. The unavailability of visual comparison for PF approximations with more than three objectives: When the number of objectives of PF approximations is more than three, visual and intuitive quality indicator can be misleading or even impossible, even though it is a prevailing comparison tool in the literature [32].
2. A compared set needed: Many indicators can only be used when compared two or more PF approximations, which makes it difficult for online investigations of a many-objective optimizer during its optimization process. In fact, the indicator that works on unary approximation not only can conduct offline estimations of the quality of an PF approximation, but also can be used to guide the selection in MOEAs in an online manner [3,5,48].
3. The lack of a reference set as a substitution of the real PF: The number of points required to accurately approximate the PF grows exponentially with more objectives. Thus, the choice of appropriate representative Pareto optimal solutions becomes an increasingly difficult task. Even worse, the true shapes and distributions of PFs are usually unknown beforehand for real-world MOPs.
4. Escalating time and space complexity: More objectives result in an exponential increase on the time and space complexity for some commonly used indicators, such as Hypervolume [49], diversity measure [14] and hyperarea difference [42]. In fact, the high space and time complexity not only limit their applicability in offline performance comparisons of high-dimensional PF approximations obtained by various many-objective optimizers, but also make it inappropriate for online evaluations of the performance of a single many-objective optimizer.

In the literature, a variety of convergence indicators have been proposed to avoid the aforementioned challenges. For this purpose, either the characteristics of the PFs in the considered test problems [26,41] or the dominance relations between the individuals [10,47] are utilized. Nevertheless, the diversity indicator seems much more difficult to design for appropriately reflecting the distribution of the approximations in many-objective optimization [39]. Over the recent years, the indicators that consider both diversity and convergence, such as Hypervolume (HV) [49] and Inverted Generational Distance (IGD) [6], are very popular in the multiobjective evolutionary optimization community [5,25,45]. IGD and HV can be defined as follows.

- Inverted Generational Distance (IGD) [6]: Let P^* be a set of points uniformly sampled over the true PF, and S be the set of solutions obtained by an EMO algorithm. The IGD value of S is computed as:

$$IGD(S, P^*) = \frac{\sum_{x \in P^*} dist(x, S)}{|P^*|} \tag{2}$$

  where $dist(x, S)$ is the Euclidean distance between a point $x \in P^*$ and its nearest neighbor in S, and $|P^*|$ is the cardinality of P^*. The lower is the IGD value, the better is the quality of S for approximating the whole PF.
- Hypervolume (HV) [49]: Let $r^* = (r_1^*, r_2^*, \ldots, r_m^*)^T$ be a reference point in the objective space that dominated by all solutions in a PF approximation S. HV metric measures the size of the objective space dominated by the solutions in S and bounded by r^*.

$$HV(S) = VOL(\bigcup_{x \in S}[f_1(x), r_1^*] \times \ldots [f_m(x), r_m^*]) \tag{3}$$

  where $VOL(\bullet)$ indicates the Lebesgue measure. Hypervolume can measure the approximation in terms of both diversity and convergency. The larger is the HV value, the better is the quality of S for approximating the whole PF.

[1] In the case of maximization, the inequality signs should be reversed.

Nevertheless, certain prerequisites must be satisfied before using these metrics, which limits their applications on estimating the diversity of high-dimensional PFs. For instance, although Monte Carlo sampling-based approximation can significantly reduce the computational cost of HV [3] and makes it possible to use for high-dimensional PFs, the proper choice of the reference point when calculating the value of HV can largely affect its accuracy [1]. Similarly, a reference set that can well-represent PF is required to calculate IGD. HV, IGD and a recent one, i.e. a reference vector based metric (p-metric) [20] measure an overall performance of convergence and diversity. However, they are unable to separately reflect the distribution of approximations. Such a characteristic may be desirable for the users to understand the diversity performance of an optimizer in an offline manner [50] or even use the diversity information to guide the selection of solutions in an online manner.

In this paper, we propose a diversity indicator based on reference vectors (DIR) for many-objective optimization. 1) A reference vector can be considered as a representative of a subregion in the objective space. The number of reference vectors a solution covers can be used to roughly estimate the coverage of such solution in an approximation. 2) Both the overall spread and uniformity of an approximation can be measured by the standard deviation of the coverage of all the solutions in an approximation. These motivations have been further discussed in Section 3.5. As DIR is a unary indicator which does not needs any compared approximation or the substitution of a PF, it is able to either conduct an offline measurement for the performance of a single many-objective optimizer or an online measurement to guide the selection of solutions for a many-objective optimizer.

The rest of this paper is organized as follows. Previous work on diversity indicators is summarized in Section 2. Section 3 elaborates DIR. In Section 4, the systematic experiments are conducted to verify the effects of DIR. In Section 5, DIR is integrated into a classical Pareto-dominance-based MOEA, NSGA-II, to enhance its performance for MaOPs. Finally, Section 6 concludes this paper.

2. Previous work

This section discusses the existing diversity indicators in the literature. Some diversity indicators only focus on a single aspect (i.e., spread or uniformity) of the diversity for PF approximations. Indicators considering only spread include

- Metric of extent ($M(S)$) [46]: It is to calculate the sum of maximal difference value of each objective, using Eq. (4).

$$M(S) = \sqrt{\sum_{i=1}^{m} max(\|x_i - y_i\|)}, \forall x, y \in S \tag{4}$$

  where S is a PF approximation; m is the number of objectives; x_i denotes the i-th objective of a solution x and y_i denotes the i-th objective of a solution y. A higher $M(S)$ value indicates a wider spread of the approximation.
- Overall Pareto spread [42]: It is defined as the volume ratio of two hypercubes. The one is defined by the best and worst solutions with respect to each objective and the other hypercube is defined by the extreme solutions of the tested PF approximation.
- Spread assessment metric [34]: It is a spread metric by using boundaries of a PF approximation. It projects the boundary solutions to the low-dimensional spaces to evaluate the extent.

Indicators dealing only uniformity include:

- Uniform distribution UD [40]: It evaluates the uniformity of an approximation S as follows:

$$UD(S) = \frac{1}{1 + Q_{sd}} \tag{5}$$

  where Q_{sd} is the standard deviation of niche counts for all solutions in S.
- Spacing [4]: It can be defined as:

$$Spacing = \sqrt{\frac{1}{|S|}\sum_{i=1}^{|S|}(d_i - d)^2} \tag{6}$$

  where S is the tested set and $d_i = min_{k\in S \wedge k\neq i} \sum_{t=1}^{m} \left|f_t^i - f_t^k\right|$, where f_t^i and f_t^k is the t-th objective value of ith or kth solution; and d is the mean of all d_is.
- Cluster [42]: It puts all the solutions into the hyperboxes and the uniformity is calculated by the ratio of the number of solutions and the hyperboxes occupied by solutions.
- Uniform assessment [35]: It constructs a minimum spanning tree (MST) for all the PF solutions. The distribution of neighboring solutions are estimated by MST for uniformity.

Although these indicators can correctly evaluate the diversity in either spread or uniformity, they may fail to reflect the whole distribution of a PF approximation [32] as exemplified in Fig. 1. In this example, all the solutions in the approximation are uniformly distributed on the boundaries of PF rather than covering the whole PF [32]. Such approximation is considered to have good diversity evaluated by either a spread or uniformity indicator, as the uniformity indicator only considers the

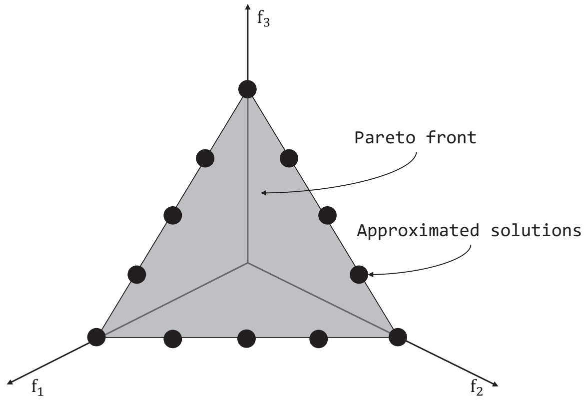

Fig. 1. An illustration of a PF approximation that is located on the boundaries of the real PF. Either spread or uniformity indicator fails to give the right evaluation of diversity in this case.

uniformity among the neighboring solutions and the spread indicator only measures the ranges of the boundary solutions. Note that for accuracy, in the remainder of the paper, spread is replaced with "coverage" to refer to the performance of an approximation to cover the whole PF, as spread only refers to the outward extension but the coverage considers both inward and outward extensions of an approximation.

Another category of the diversity indicators considers both coverage and uniformity as a whole.

1. Δ Metric [16] measures the diversity of the approximation P as follows.

$$\Delta = \frac{d_f + d_l + \sum_{i=1}^{N-1} \left| d_i - \overline{d} \right|}{d_f + d_l + (N-1)\overline{d}} \tag{7}$$

   where d_f and d_l are the Euclidean distances between extreme solution of the PF and the boundary solutions in the approximation regarding each objective, respectively. N denotes the size of the approximation P. d_i, where $i = 1, 2, \ldots, N-1$, denotes the Euclidean distance between consecutive solutions in P and $\overline{d}$ is the average of all d_i. Δ Metric is mainly designed to estimate the diversity of an approximation in a bi-objective problem although it can be extended to evaluate a high dimensional approximation by using Voronoi diagram approach. However, finding the Voronoi diagram of a solution set is a very difficult (or even an infeasible) task when more than three objectives are involved [2,32].
2. Sigma Diversity Metric (SDM) [38] computes the angular positions of solutions in an approximation in the objective space divided by a set of reference vectors. The outputs of SDM are a percentage of the space and the position information of a given approximation in the space rather than a scalar value. However, SDM is difficult to be extended to many-objective optimization, as it depends on several parameters, such as the distance around each reference line, the number of reference line, and the shape of the PF.
3. Diversity Metric (DM) [14] measures the diversity by comparing the PF approximation with a reference set. To calculate the DM, solutions in the approximation are projected on a $(m-1)$-dimensional hyperplane which is divided into a number of hyperboxes. The indicator considers each hyperbox and gives it an evaluated value based on both the distribution of the solutions in it and its neighbors. The more the hyperbox that contain both a member of the reference set and a member of the approximation simultaneously, the higher the indicator value is. However, DM needs to access each hyperbox to estimate the distribution, which greatly increase its computational cost. In addition, DM needs to use a reference set, in which the solutions are uniformly distributed over the PF. However, the requirement that the number of solutions in the reference set is equal to the number of solutions in the approximation becomes an obstacle for DM to be used for high-dimensional approximation. In addition, the requirement of a reference set makes it difficult to be used as an online indicator.
4. Diversity Comparison Indicator (DCI) [32] evaluates the relative quality of different PF approximations rather than provides an absolute measure of distribution. The underlying idea behind the DCI is to consider the contribution of different PF approximations to the hyperboxes that have at least one nondominated solution. All the concerned approximations are put into a number of hyperboxes and DCI is a value that reflects the contribution of each approximation to the hyperboxes that have at least one nondominated solution. Therefore, the number of hyperboxes is very likely to affect the precision of DCI. In addition, DCI only works when comparing multiple approximations, which makes it difficult to be used as an online indicator.
5. Online Diversity Metric [19] is an online diversity assessment to measure the diversity loss caused by any individual in the population. But unfortunately, it can only be applied to a single individual rather than the whole PF approximation.

Table 1
The comparison between previous indicators and proposed indicator.

Diversity indicator	Δ metric	SDM	DM	DCI	DIR
A substitution of PF needed	✓		✓		
Difficult for high dimensional PFs	✓		✓		
Parameters to be tuned		✓		✓	
The number of approximations	unary	unary	unary	multivariate	unary
The number of metric values	single	multiple	single	single	single
Computational effect	quadratic	linear time	exponential in m	quadratic	quadratic

Major properties of the existing diversity indicators and our proposed DIR are summarized in Table 1. As it can be observed that, unlike Δ metric and DM, DIR does not require a substitution of PF, besides that it can work well for high dimensional PF approximation. Different from DCI and SDM, where a parameter needs to be tuned carefully, DIR is parameterless. In addition, DIR is a unary metric with relatively low computational cost, which makes it practical as an online indicator for many-objective optimizers.

3. The diversity indicator based on reference vectors

In this section, DIR is detailed as follows. For a m-objective optimization problem, given a Pareto approximation S ($|S| = N$), DIR is used to estimate the diversity of S.

3.1. The framework of calculating DIR

The main procedure to calculate DIR is presented in Algorithm 1. Firstly, a set of M reference vectors are generated, each

Algorithm 1: Diversity indicator based on reference vectors (DIR).

```
Input: S = {s^1, s^2, ..., s^N};
Output: DIR;
Step 1 The initialization of reference vectors:
1 Initialize V = {λ^1, λ^2, ..., λ^M};
Step 2 Computing the coverage vector based on reference vectors:
2 c = Computing_coverage(S, V);
Step 3: Computing DIR based on coverage vector:
3 DIR = Computing_DIR(c);
4 return DIR;
```

of which is a representative of the subregion in the objective space. Then, the coverage of each solution in S is calculated based on reference vectors and stored in a coverage vector $c = (c_1, c_2, \ldots, c_N)^T$ in S. Lastly, DIR is estimated by evaluating the standard deviation of c. Each step is detailed in the following sections.

3.2. The initialization of reference vectors

To implement DIR, a set of reference vectors V ($|V| = M$), each of which represents a subregion in the objective space, is firstly generated either by uniform generation [11] or two-layered generation of reference vectors [13].

3.3. Computing the coverage vector based on the reference vectors

The evaluation of coverage for all the solutions is presented in Algorithm 2. For each reference vector, it finds its closest solution. The closeness between a reference vector λ^i and a solution s^j is defined by:

$$angle(\lambda^i, F(s^j)) = \arccos(\frac{(\lambda^i)^T \cdot (F(s^j) - z^*)}{\|\lambda^i\| \|F(s^j) - z^*\|}) \tag{8}$$

where $z^* = (z_1^*, z_2^*, \ldots, z_m^*)^T$ is the ideal objective vector with $z_i^* = \min_{x \in \Omega} f_i(x), i \in \{1, 2, \ldots, m\}$.

If a reference vector λ^i is closest to a solution s^j, we say that solution s^j covers the reference vector λ^i. More precisely speaking, solution s^j covers the subregion that the reference vector λ^i represents. The coverage vector c is used to record the number of reference vectors covered by each solution, where c_i denotes the number of reference vectors covered by the ith solution.

In Algorithm 2, each reference vector λ^i finds its closest solution s^{minsub} based on Eq. (8) (lines 4–10), where $minsub$ is the index of the closest solution. The coverage of solution s^{minsub}, denoted by c_{minsub}, is incremented by one accordingly.

Algorithm 2: Computing_coverage(S, V).

Input : $S = \{s^1, s^2, \ldots, s^N\}$;
Reference vectors $V = \{\lambda^1, \lambda^2, \ldots, \lambda^M\}$;
Output: c.

Initialize $c : (c_1, c_2, \ldots, c_N)^T$, and each $c_i = 0$;
for $i = 1; i <= M; i++$ **do**
    $minsub = +\infty, minangle = +\infty$;
    for *each solution* s^j *in* S **do**
        $\theta_j = angle(\lambda^i, F(s^j))$;
        if $\theta_j < minangle$ **then**
            $minsub = j$;
            $minangle = \theta_j$;
        end
    end
    $c_{minsub} = c_{minsub} + 1$;
end
return c;

3.4. Computing DIR based on the coverage vector

The DIR of the whole approximation, for both coverage and uniformity, can be estimated by evaluating the standard deviation of $c = (c_1, c_2, \ldots, c_N)^T$ according to Eq. (9), where $mean(c)$ is the average value of c.

$$DIR^* = std(c) = \sqrt{\frac{1}{N}\sum_{i=1}^{N}(c_i - mean(c))^2} \tag{9}$$

Note that in the best case where the approximation is evenly and widely spread in the objective space, the value of DIR is 0, which represents each solution covers the same number of reference vectors. In the worst case, one solution covers all M reference vectors and the rest solutions covers no reference vectors and the coverage vector becomes $c = (M, 0, \ldots, 0)^T$. The maximum DIR value in the worst is $std(c) = \sqrt{\frac{1}{N}\left[\left(M - \frac{M}{N}\right)^2 + (N-1)\frac{M^2}{N^2})\right]}$, which can be simplified as:

$$DIR_{max} = \frac{M}{N}\sqrt{N-1} \tag{10}$$

Therefore, it is clear to know that DIR value ranges from 0 to $\frac{M}{N}\sqrt{N-1}$ and the normalized DIR is as follows:

$$DIR = \frac{DIR^*}{DIR_{max}} = \frac{\sqrt{\frac{1}{N}\sum_{i=1}^{N}(c_i - mean(c))^2}}{\frac{M}{N}\sqrt{N-1}} \tag{11}$$

All above procedures computing DIR based on coverage vector are given in Algorithm 3.

Algorithm 3: Computing_DIR(c).

Input: $c : \{c_1, c_2, \ldots, c_N\}$
Output: DIR.

$DIR^* = std(c)$;
$DIR_{\max} = \frac{M}{N}\sqrt{N-1}$;
$DIR = \frac{DIR^*}{DIR_{\max}}$;
return DIR;

3.5. DIR for three typical PF approximations

Fig. 2 provides three typical PF approximations for further explaining DIR. Among them, Fig. 2(a) shows a PF approximation with the ideal distribution. In Fig. 2(a), each solution covers one subregion represented by one reference vector. Therefore, the coverage vector of such PF approximation is $c = (1, 1, 1, 1, 1, 1)^T$ and DIR value is equal to 0 (the best case). Fig. 2(b) shows a PF approximation with good coverage but bad uniformity. It is clear to see that the coverage vector of

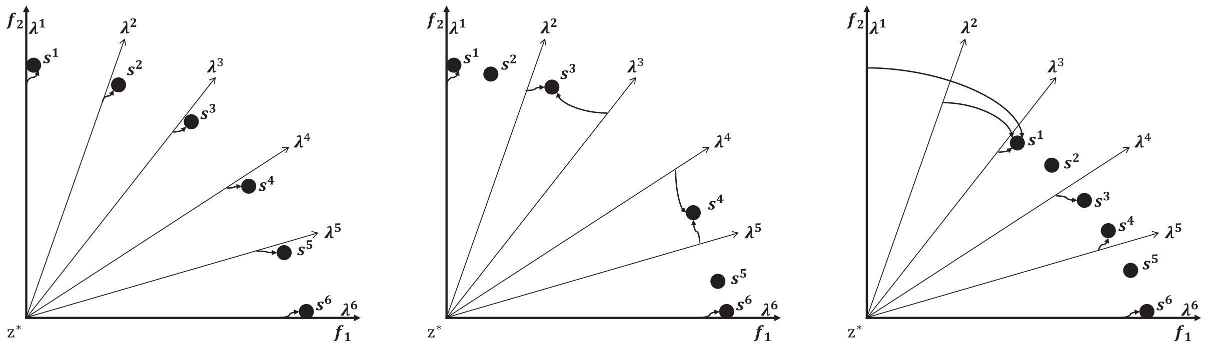

(a) A PF approximation with the ideal distribution. Its coverage vector is $c = (1, 1, 1, 1, 1, 1)^T$ and DIR value is 0.

(b) A PF approximation with good coverage but bad uniformity. Its coverage vector is $c = (1, 0, 2, 2, 0, 1)^T$ and DIR value is 0.3651.

(c) A PF approximation with limited coverage. Its coverage vector is $c = (3, 0, 1, 1, 0, 1)^T$ and DIR value is 0.4472.

Fig. 2. Examples of DIR on MaOPs with different PF approximations.

such PF approximation is $c = (1, 0, 2, 2, 0, 1)^T$ and its corresponding DIR value is 0.3651. In the third case, the PF approximation does not cover all the objective regions, as shown in Fig. 2(c). It can be observed that the coverage vector of such PF approximation is $c = (3, 0, 1, 1, 0, 1)^T$ and DIR value is 0.4472.

Three typical PF approximations and their corresponding DIR values indicate that DIR is able to reflect both the coverage and uniformity for a PF approximation. The smaller the DIR, the better the diversity of a PF approximation is.

3.6. Discussions on the accuracy of DIR

Given the limited number of reference vectors (M), DIR may have accuracy limit, which can be explained as follows. Fig. 3(a) shows the coverage vector and the DIR value of an evenly distributed PF approximation S_1 with $M = 6$ reference vectors; and Fig. 3(d) shows the coverage vectors and the DIR value of an unevenly distributed PF approximation S_2, also with $M = 6$ reference vectors. Although the coverage vectors and the DIR values of S_1 and S_2 are the same when $M = 6$ reference vectors are used for computing DIR, it is apparent that the actual diversity of S_2 in Fig. 3(d) is worse than that of S_1 in Fig. 3(a).

The accuracy of the DIR for PF approximations can be improved by simply increasing the number of reference vectors. For the PF approximation S_1 but with $M = 11$ reference vectors (Fig. 3(b)), its coverage vectors becomes $(2, 2, 2, 2, 2, 1)^T$ and DIR value is 0.0909. For the same PF approximation S_2 with $M = 11$ reference vectors (Fig. 3(e)), its coverage vectors becomes $(2, 1, 2, 3, 2, 1)^T$ and DIR values is 0.1676. It is clear to see that DIR values with $M = 11$ reference vectors already successfully reflect the actual diversity of these two PF approximations, as the DIR value of S_1 is lower (better) than that of S_2. In fact, when M becomes a positively infinite number, the coverage of one solution can be seen as the hypercone volume covered by such a solution, as shown in Fig. 3(c) and (f). It can be seen clearly that the more differently these hypercone volumes vary from each other, the higher DIR value of a PF approximation is (i.e. the worse diversity).

3.7. More discussions on DIR and p*-metric*

p-metric [20] is a recently proposed performance indicator for high-dimensional PF approximations. It divides the objective space into subregions of hypercones by reference vectors. A solution s belongs to i-th subregion Φ_i if $i = argmax_{\lambda^i \in V} \frac{(\lambda^i)^T \cdot F(s)}{\|\lambda^i\| \|F(s)\|}$, where λ^i is the i-th reference vector and $F(s)$ is the objective vector of the solution s. In each subregion Φ_i, the solution that has the closest distance r_i to the origin point, is tracked and used to define p-metric, as follows.

$$p\text{-metric} = \sum_{i=1}^{M} \frac{1}{r_i} \tag{12}$$

where M is the number of subregions and $\frac{1}{r} = 0$ for the subregion containing no solution. It is clear to see from Eq. (12) that the diversity of a PF approximation, in terms of the p-metric, is measured by the number of reference vectors (subregions) that have the associated solution(s).

In this section, the differences of DIR and p-metric are discussed as follows.

1. p-metric is a comprehensive indicator that considers both convergence and diversity while DIR is a diversity indicator.
2. For a PF approximation with N solutions and limited M reference vectors, both DIR and p-metric have their accuracy limits. However, different from p-metric, the accuracy of DIR can be improved by increasing M, as described in the last

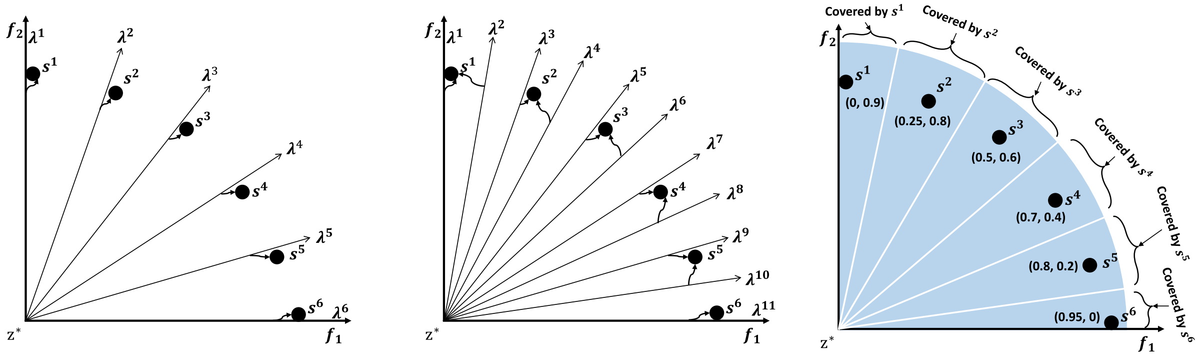

(a) Evenly distributed PF approximation S_1 with $M = 6$ reference vectors. Its coverage vector is $(1, 1, 1, 1, 1, 1)^T$ and DIR value is 0.

(b) Evenly distributed PF approximation S_1 with $M = 11$ reference vectors. Its coverage vector is $(2, 2, 2, 2, 2, 1)^T$ and DIR value is 0.0909.

(c) Evenly distributed PF approximation S_1 with $M = infinite$ reference vectors.

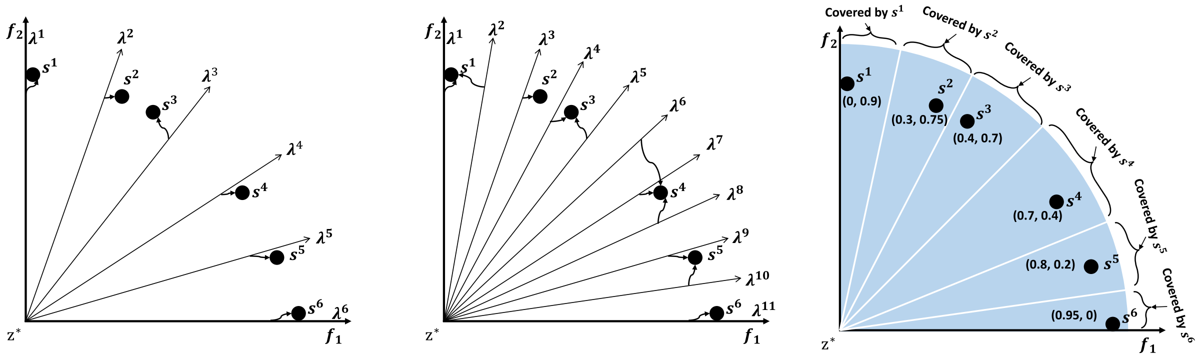

(d) Unevenly distributed PF approximation S_2 with $M = 6$ reference vectors. It coverage vector is $(1, 1, 1, 1, 1, 1)^T$ and DIR value is 0.

(e) Unevenly distributed PF approximation S_2 with $M = 11$ reference vectors. Its coverage vector is $(2, 1, 2, 3, 2, 1)^T$ and DIR value is 0.1676.

(f) Unevenly distributed PF approximation S_2 with $M = infinite$ reference vectors.

Fig. 3. An illustration of two PF approximations and their corresponding DIR values with $M = 6, 11$ and *infinite* reference vectors.

section. This is due to their fundamentally different ways in associating solutions with reference vectors (or located subregions). In DIR, each reference vector finds its nearest solution while in *p*-metric, each solution finds its closest reference vector (or its located subregion). In other words, for DIR, one solution can be associated with multiple reference vectors and one reference vector can associate with only one solution. On the contrary, for *p*-metric, one solution can be located in only one subregion and one subregion may contain multiple solutions. Its accuracy cannot be improved by increasing *M*, as *N* solutions can be at most located in *N* subregions.

3.8. Computational cost of DIR

In the Step 1 of Algorithm 1, generating *M* reference vectors requires $O(M)$ computations. Step 2 requires $O(mNM)$ to compute coverage for all solutions. In Step 3, $O(N)$ is needed to calculate standard deviation of the coverage vector. In summary, the computational complexity of DIR is $O(mNM)$, where *M* is the number of reference vectors, *N* is the number of solutions in a PF approximation and *m* is the number of objectives.

4. Experiments and discussions

In this section, we conduct experiments to validate DIR on both artificially generated PF approximations and the ones obtained by seven many-objective optimizers. The effects of the number of reference vectors on DIR are also discussed in this section.

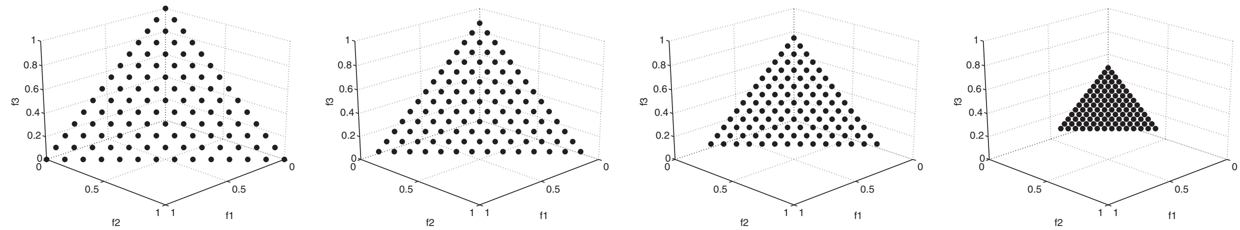

(a) Every objective value of the PF approximation ranges in $[0, 1]$, and its obtained DIR is 0.00000

(b) Every objective value of the PF approximation ranges in $[0.05, 0.9]$ and its obtained DIR is 0.08120

(c) Every objective value of the PF approximation ranges in $[0.1, 0.8]$, and its obtained DIR is 0.08452

(d) Every objective value of the PF approximation ranges in $[0.2, 0.6]$, and its obtained DIR is 0.24472

Fig. 4. The artificial PF approximations with different coverage, uniformly located on the hyperplane $f_1 + f_2 + f_3 = 1$.

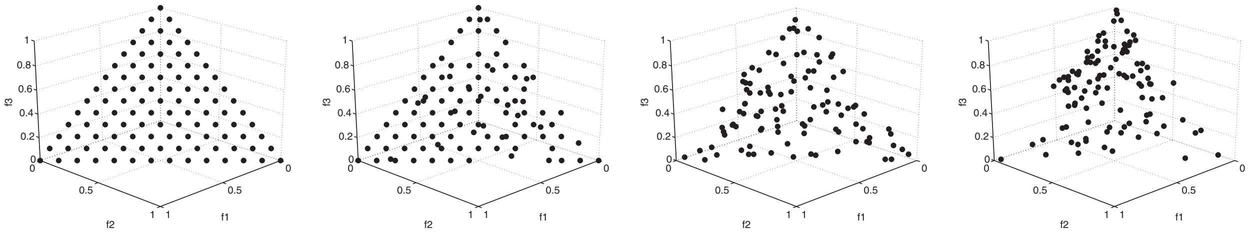

(a) DIR= 0.00000 (b) DIR= 0.05064 (c) DIR= 0.07288 (d) DIR= 0.10742

Fig. 5. The artificial PF approximations with different uniformity, located on the hyperplane $f_1 + f_2 + f_3 = 1$.

4.1. Experimental setups

The uniform generation of reference vectors [11] is adopted for 3-, 4- and 5-dimensional PF approximations; and multi-layered generation of reference vectors [13] is used for 8- and 10-dimensional PF approximations. For convenience, the number of reference vectors M is set to N without specification.

4.2. DIR on artificial PF approximations

Two groups of artificially generated approximations are generated and presented in Figs. 4 and 5, respectively. All approximations are located on the hyperplane $f_1 + f_2 + f_3 = 1$ and each approximation contains $N = 105$ solutions. In the first group of the artificial PF approximations, all the approximations are uniformly distributed but the coverage of them is very different from each other. In Fig. 4a, every objective value of all the solutions ranges in [01]. In Fig. 4(b), every objective value of all the solutions ranges in [0.05, 0.9]. In Fig. 4(c), every objective value of all solutions ranges in [0.1, 0.8]. In Fig. 4(d), every objective value of all solutions ranges in [0.2, 0.6]. It can be observed from these figures that the wider distribution of an approximation, the smaller DIR value it has, which indicates that DIR can accurately reflect the coverage of PF approximations.

In the second group, all the approximations are distributed over the entire PF, but the uniformity of each approximation is different from each other. The approximations are generated as follows. Firstly, the solutions are uniformly generated on the plane $f_1 + f_2 + f_3 = 1$, ranging in [0, 1], as shown in Fig. 5(a). After that, when 10%, 50% or 100% of solutions are replaced with randomly generated solutions on the same plane, different solution sets can be obtained, as shown in Fig. 5(b)–(d). It can be observed in Fig. 5(a)–(d), that DIR values become increasingly larger when the uniformity of the solution sets becomes increasingly worse. Obviously, DIR can correctly reflect the uniformity of those PF approximations.

4.3. DIR on real PF approximations

In this section, DIR is used to estimate the diversity of PF approximations, obtained by seven classical MOEAs (MOEA/D-DE [30], IBEA [48], GDE3 [28], PAES [27], SPEA2+SDE [33], GrEA [43] and NSGA-III [13]) on many-objective DTLZ benchmark problems [17]. All their parameters are set as suggested in the original papers. Each optimizer is run 30 times on each instance and the approximation with the median DIR value is used for comparisons.

The population or approximation sizes for MaOPs with different number of objectives are listed in Table 2. It is noted that the population (or the solution set) in an evolutionary optimizer is used to approximate the PF of an MaOP. To avoid the confusion, the "population size" is replaced with "the approximation size", in the rest of the paper.

The selection of the approximation size for MaOPs with different number of objectives can be justified as follows. For some selected many-objective evolutionary algorithms (e.g., MOEA/D-DE [30] and NSGA-III [13]), the population size (the

Table 2
The approximation size for MaOPs with the different number of objectives.

The number of objectives	3	4	5	8	10
The approximation size	120	120	126	156	275

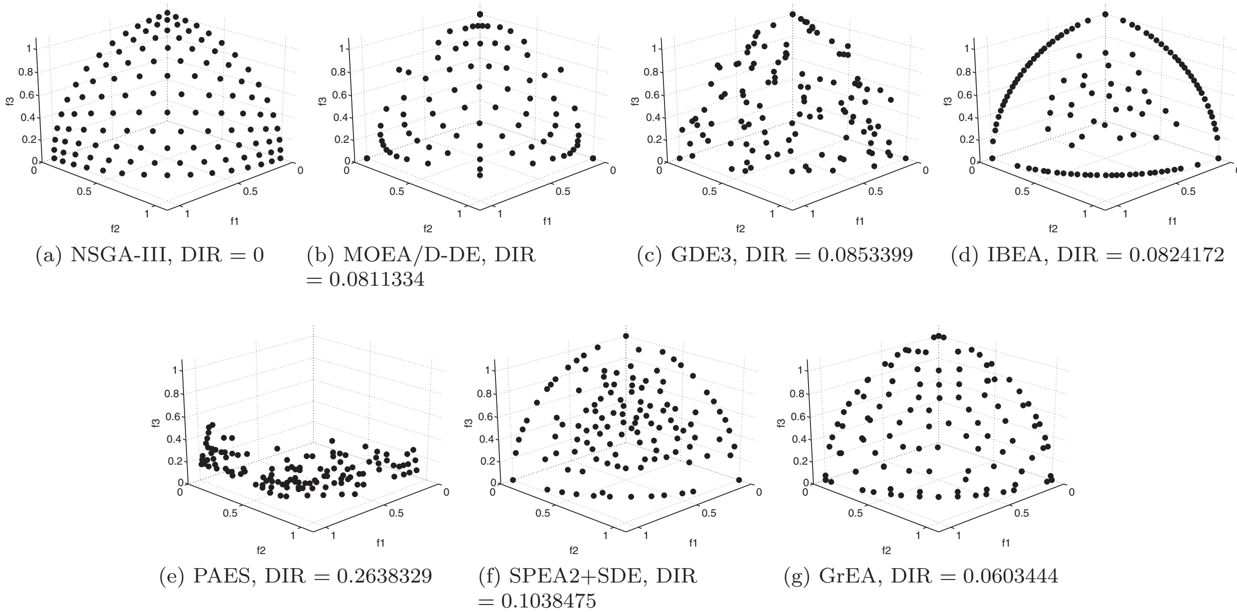

(a) NSGA-III, DIR = 0 (b) MOEA/D-DE, DIR = 0.0811334 (c) GDE3, DIR = 0.0853399 (d) IBEA, DIR = 0.0824172

(e) PAES, DIR = 0.2638329 (f) SPEA2+SDE, DIR = 0.1038475 (g) GrEA, DIR = 0.0603444

Fig. 6. PF approximations obtained by seven algorithms on 3-objective DTLZ2.

approximation) is equal to the number of reference vectors in the original paper. In NSGA-III [13], Das and Dennis's systematic approach [11] is adopted for generating reference vectors by uniformly sampling reference points on a unit simplex. In this way, the number of reference vectors (i.e., the approximation size) is

$$N = \binom{m-1}{H+m-1} \tag{13}$$

where $H > 0$ is the number of divisions along each objective coordinate and m is the number of objectives.

Based on Eq. (13), H is set to 12 or the number of reference vectors (population size) is 120 for tri-objective problems; H is set to 7 or the number of reference vectors (population size) is 120 for 4-objective problems; and H is set to 5 or the number of reference vectors (population size) is 126 for 5-objective problems.

However, the direct use of Das and Dennis's approach may not suite for MaOPs with more than 6 objectives [13]. This can be explained as follows. As long as $H \geq m$ is not chosen, no intermediate reference points on the simplex will be created by Das and Dennis's approach. In other words, all the generated reference vectors only have the intersecting reference points on the boundaries of the unit simplex. For MaOPs with more than 6 objectives, setting $H \geq m$ leads to a huge number of reference vectors, based on Eq. (13). For example, for a 7-objective problem, $H = 7$ results in $\binom{7-1}{7+7-1} = 1716$ reference vectors. To avoid such a situation, two layers including a boundary layer and an inside layer of reference points are used in [13,31] for MaOPs with more than 6 objectives. As suggested in [13,31], we use $H = 3$ and $H = 2$ for boundary and inside layers, respectively, thereby requiring a total of $\binom{8-1}{3+8-1} + \binom{8-1}{2+8-1} = 156$ reference vectors for 8-objective problems and $\binom{10-1}{3+10-1} + \binom{10-1}{2+10-1} = 275$ reference vectors for 10-objective problems.

DTLZ2 [17], that has a regular PF, is selected to verify the effectiveness of DIR. All the optimizers are relatively easy to converge to the PF of the DTLZ2. This is very helpful to test the diversity of the approximation sets obtained by the different optimizers.

The PF approximations obtained by seven algorithms on 3-objective DTLZ2 are plotted in Fig 6 and the parallel coordinate plots of seven approximations for 5- and 10-objective DTLZ2 are plotted in Figs. 7 and 8, respectively. The corresponding DIR values for them are listed in Table 3.

For 3-objective DTLZ2, it can be seen in Fig 6 that the approximation obtained NSGA-III has the best (lowest) DIR value (0). GrEA delivers the second best DIR value as its obtained approximation is well-spread although not as uniform as the one obtained by NSGA-III. The DIR values of the approximations obtained by IBEA and MOEA/D-DE are similar. The approx-

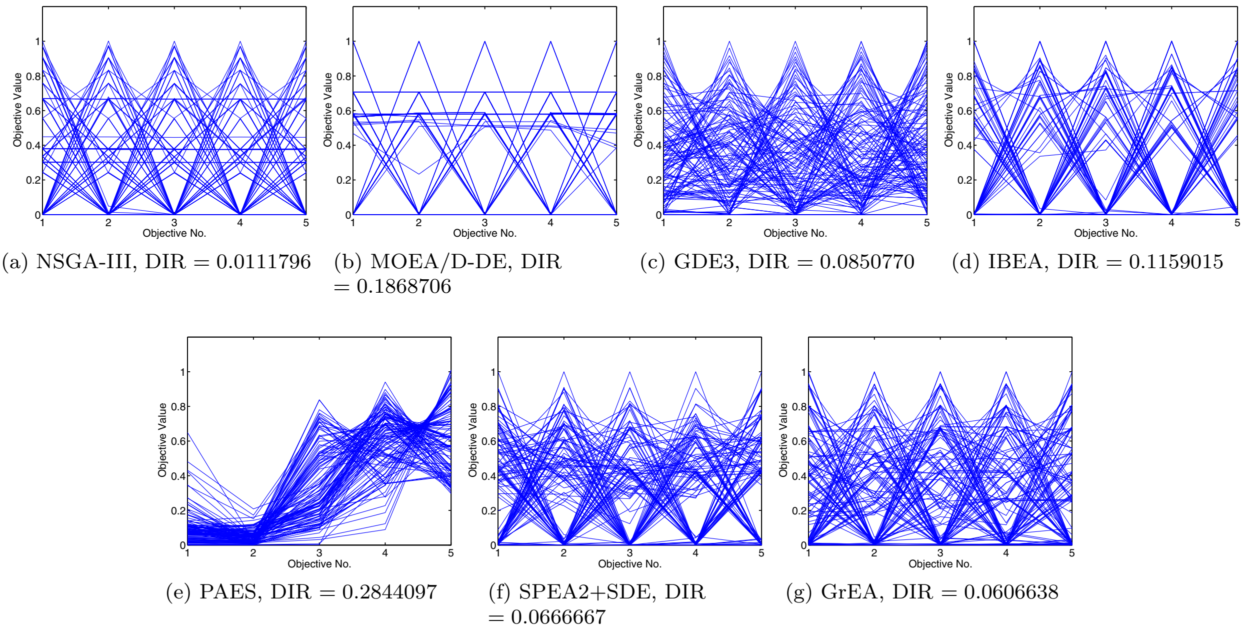

(a) NSGA-III, DIR = 0.0111796 (b) MOEA/D-DE, DIR = 0.1868706 (c) GDE3, DIR = 0.0850770 (d) IBEA, DIR = 0.1159015

(e) PAES, DIR = 0.2844097 (f) SPEA2+SDE, DIR = 0.0666667 (g) GrEA, DIR = 0.0606638

Fig. 7. Parallel coordinate plots obtained by seven algorithms on 5-objective DTLZ2.

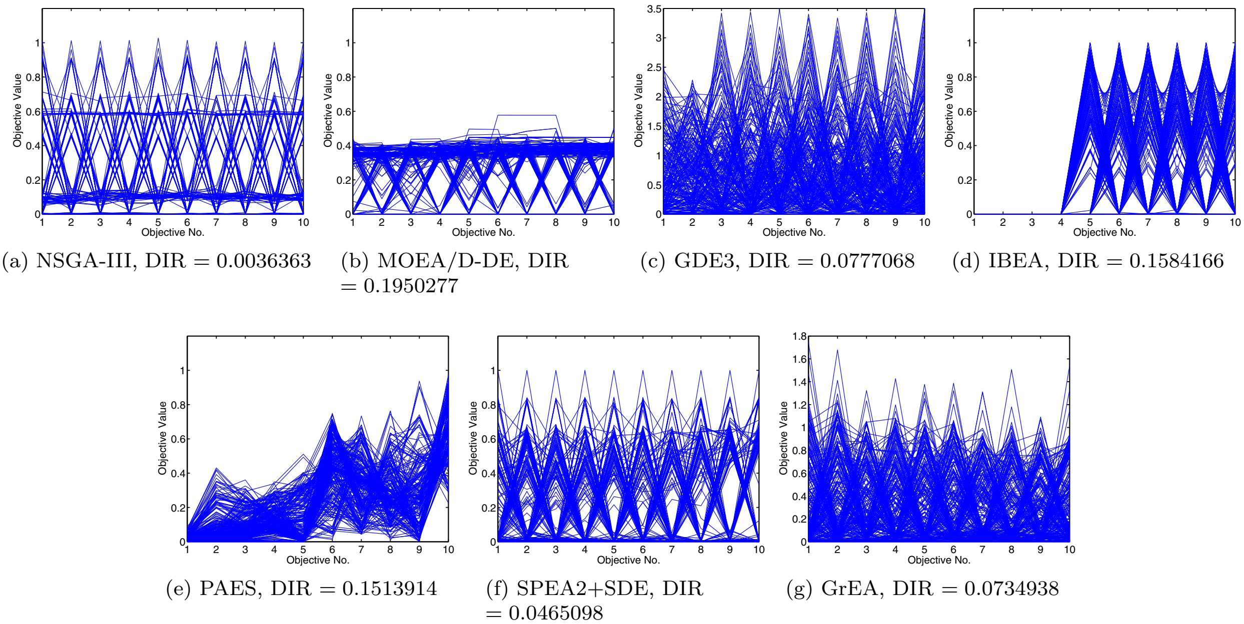

(a) NSGA-III, DIR = 0.0036363 (b) MOEA/D-DE, DIR = 0.1950277 (c) GDE3, DIR = 0.0777068 (d) IBEA, DIR = 0.1584166

(e) PAES, DIR = 0.1513914 (f) SPEA2+SDE, DIR = 0.0465098 (g) GrEA, DIR = 0.0734938

Fig. 8. Parallel coordinate plots obtained by seven algorithms on 10-objective DTLZ2.

Table 3
DIR for PF approximations with different number of objectives obtained by seven algorithms.

the number of objectives	NSGA-III	MOEA/D-DE	GDE3	IBEA	PAES	SPEA+SDE	GrEA
3	0	0.0811334	0.0853399	0.0824172	0.2638329	0.1038475	0.0603444
4	0	0.1429971	0.0828417	0.0776041	0.3424976	0.0843384	0.0668060
5	0.0111796	0.1868706	0.0853399	0.1159015	0.2844097	0.0666667	0.0606638
8	0	0.2244375	0.1076096	0.1132277	0.2890331	0.0622496	0.0749966
10	0.0036363	0.1950277	0.0777068	0.1584166	0.1513914	0.0465098	0.0734938

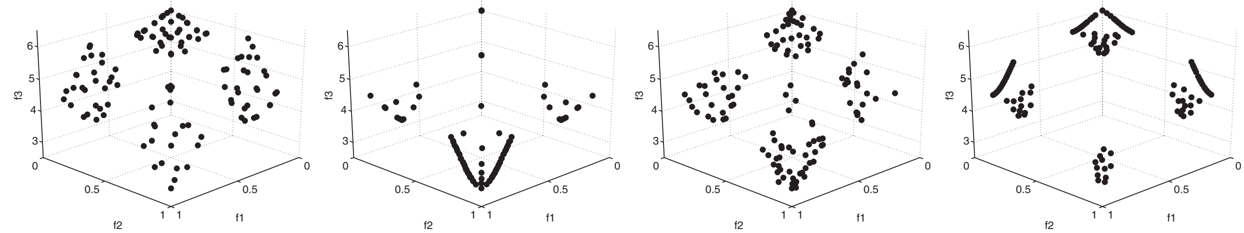

(a) NSGA-III, DIR = 0.1201073 (b) MOEA/D-DE, DIR = 0.2770392 (c) GDE3, DIR = 0.1547565 (d) IBEA, DIR = 0.1763286

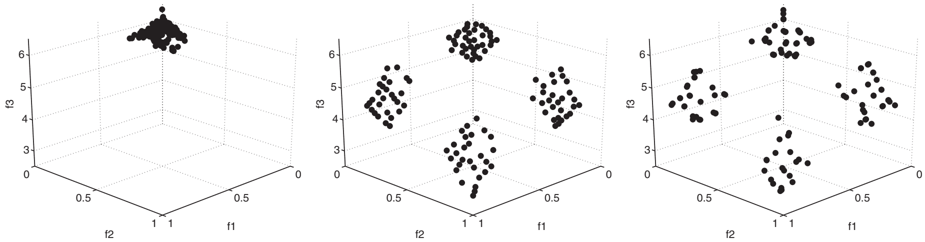

(e) PAES, DIR = 0.5751629 (f) SPEA2+SDE, DIR = 0.1473387 (g) GrEA, DIR = 0.1719064

Fig. 9. PF approximations obtained by seven optimizers on 3-objective DTLZ7 problem.

imation obtained by IBEA is distributed more uniformly but the approximation obtained by MOEA/D-DE is distributed more widely. This observation is consistent with the fact that most of the solutions obtained by IBEA are uniformly distributed only on the boundary of the real PF without proper coverage inside the PF while the solutions obtained by MOEA/D-DE are located over the whole PF without good uniformity. The PF approximation obtained by GDE3 is less uniformly distributed than that obtained by MOEA/D-DE and thus it has an even worse DIR value. The approximation obtained by SPEA2+SDE is very similar to that of IBEA. However, the uniformity of solutions obtained by SPEA2+SDE is worse than that of IBEA which leads to a worse (higher) DIR value. The approximation obtained by PAES has the worst diversity in terms of both coverage and uniformity which leads to a worst (highest) DIR value. Fig. 7 shows the approximations obtained by 7 optimizers on 5-objective problems. NSGA-III, according to parallel coordinates [22], has the best performance and lowest DIR value (0.0111796). Meanwhile, the approximation obtained by GrEA is not distributed uniformly enough so it has a worse DIR value (0.06066388). For SPEA2+SDE (DIR = 0.0666667), as shown in Fig. 7(f), its approximation is distributed less widely and uniformly than that of GrEA. The approximation obtained by IBEA (DIR = 0.1159015) is more uniformly distributed but covers less regions than that obtained by GDE3 (DIR = 0.0850770). MOEA/D-DE (DIR = 0.1868706) and PAES (DIR = 0.2844097) perform worse than other compared algorithms, based on their DIR values, as the approximation of MOEA/D-DE concentrates on the several small regions and the approximation of PAES misses some boundary regions of the PF. Similar results can be observed on approximations for 10-objective DTLZ2, as shown in Fig. 8. From the above observations, DIR is obviously able to correctly reflect the diversity of the PF approximations obtained by seven different algorithms.

4.4. DIR on MaOPs with irregular PFs

In this section, we further validate the effectiveness of DIR on MaOPs with irregular PFs. DTLZ7 is a typical irregular problem, consisting of 2^{m-1} disconnected PFs, whose shapes may be either convex or concave.

The approximations and the corresponding DIR values obtained by seven algorithms on DTLZ7 are shown in Fig. 9. It can be observed that NSGA-III has the best (lowest) DIR value (0.1201073) due to its best coverage and SPEA2+SDE has the second best DIR value (0.1473387) as the solutions it produces are uniformly distributed. The DIR value obtained by GDE3 (0.1547565), GrEA (0.1719064) and IBEA (0.1763286) are worse than that of SPEA2 + SDE due to either worse coverage or uniformity of approximations obtained by them. The DIR value obtained by MOEA/D is as low as 0.2770392, because the one entire segment of PF is not well approximated by MOEA/D. The DIR value (0.5751629) obtained by PAES is the worst, as PAES fails to approximate four segments of PF. The values of DIR on different approximations are consistent with our observations in Fig. 9, which validates the effectiveness of DIR on MaOPs with irregular PFs.

It is worth to note that DIR prefers more on coverage than uniformity for MaOPs with irregular PFs. This phenomenon can be explained as follows. As many reference vectors have no interactions with the irregular PF (e.g., the PF of DTLZ7), the boundary solutions are likely to cover a great number of such reference vectors and thus these boundary solutions are more biased when calculating DIR.

Table 4
DIR on different number of reference vectors.

Divisions (H)	The number of reference vectors	IBEA	MOEA/D-DE	GDE3	NSGA-III	PAES	SPEA2+SDE	GrEA
2	15	0.24226	0.24331	0.24331	0.24355	0.32249	0.24331	0.24355
4	70	0.14381	0.17038	0.10453	0.08077	0.27926	0.08253	0.08077
6	210	0.09152	0.16241	0.07251	0.04720	0.27614	0.06306	0.04720
8	495	0.08628	0.15154	0.06441	0.04628	0.28313	0.06357	0.03677
10	1001	0.08495	0.13539	0.05854	0.02842	0.28573	0.05199	0.03040
12	1820	0.08557	0.13709	0.05461	0.02194	0.29091	0.04359	0.02789
14	3060	0.08810	0.13893	0.05331	0.02417	0.29263	0.04362	0.02854
16	4845	0.08958	0.13634	0.05230	0.02522	0.29409	0.04092	0.02820

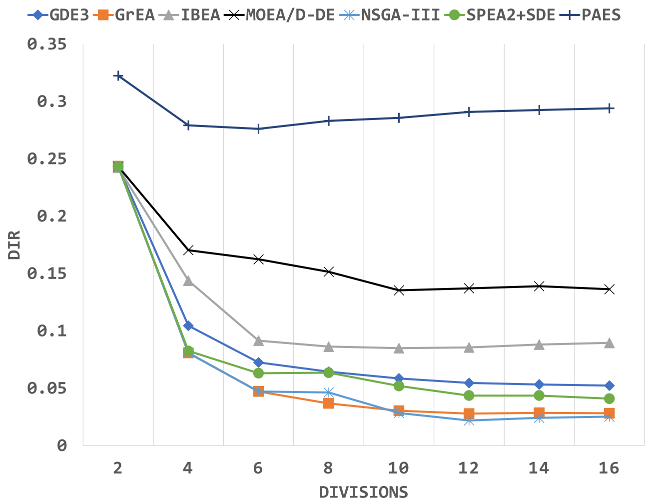

Fig. 10. DIR on different divisions.

4.5. The effects of the number of reference vectors on DIR

In this section, we investigate the effects of the number of reference vectors (M) on DIR. In the experiments, uniform generation of reference vectors is adopted and the number of vectors is controlled by changing the number of divisions H [11]. Table 4 shows the DIR values obtained by seven algorithms on 5-objective DTLZ2. For better visualization, the results of Table 4 are also plotted in Fig. 10. From Table 4 and Fig. 10, we can have the following observations.

1. DIR values gradually decline and level off with the increase of the number of reference vectors.
2. The disparities of DIR values on different approximation become larger with the increasing number of reference vectors. Therefore, the precision of DIR can be controlled by increasing the number of reference vectors.
3. The DIR values produced by GrEA slightly interwinds with that produced by NSGA-III along with the increase of the number of reference vectors. One explanation is that diversity evaluated by DIR is a tradeoff between coverage and uniformity. The preference of the two aspects for diversity may slightly change when adopting different sets of reference vectors.

To ensure that each solution in the approximation can cover at least one reference vector (subregion), the value of M (the number of reference vectors) is suggested to set to at least N (the size of the approximated set). In addition, with the increase of M, both the accuracy and the computational cost ($O(mNM)$) of DIR also increase. In other words, the selection of M depends on the appropriate balance between the accuracy and the computational cost of DIR. With the affordable computational cost, the value of M can be set as large as possible.

One possible guideline of using DIR is to set the parameter M to N initially. If DIR is not able to distinguish two approximations, then the value of M can be increased until it can distinguish the approximations or the computational cost of computing DIR values reaches the largest affordable value. The latter indicates that the diversity values of these two approximations are very close to each other.

5. A DIR-enhanced NSGA-II for MaOPs

The above empirical studies suggest DIR is an effective offline diversity metric that is able to reflect both coverage and uniformity of a PF approximation. In this section, DIR is used as an online diversity metric, which can be integrated into the selection procedure of NSGA-II [16] and further enhance its performance on MaOPs.

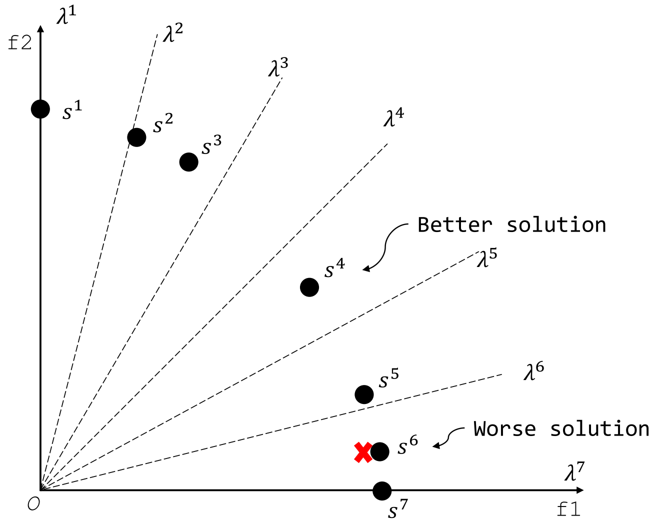

Fig. 11. An illustration of how DIR based selection works.

To avoid high computational burden, instead of selecting N solutions with the best (lowest) DIR value, a more greedy method, that selects the first N solutions covering most reference vectors, is used. Such an example is given in Fig 11, where s^4 is considered as a more diverse solution because it covers both reference vectors λ^4 and λ^5 and s^6 is regarded as a less diverse solution as it covers no reference vectors.

5.1. Integration of DIR into NSGA-II

In the DIR-enhanced NSGA-II (d-NSGA-II), all procedures are exactly the same as NSGA-II except that the crowding-distance-based estimation is replaced with DIR. The main procedure of the DIR-based selection is given in Algorithm 4.

Algorithm 4: DIR_Selection(S, F$_l$, N, V).

Input : N: The PF approximation size;
V: The reference vectors;
S: The input solution set ($|S| < N$);
$F_l = \{s_f^1, s_f^2, \ldots,\}$: The last non-domination level;

Output: S: The returned solution set ($|S| = N$).

$T = |S|$;
$U = S \bigcup F_l$;
$c = Computing\_coverage(U, V)$;
/* use Algorithm 2 to set coverage */
$c' = c[T + 1 : T + |F_l|]$;
/* copy all c values of solutions in F_l to c' */
$[c', I] = Sort(c')$;
/* sort c' in a descending order and I stores the indexes of the solutions after sorting */
for $i = 1; i \le N - T; i++$ **do**
  $S = S \bigcup \{s_f^{I_i}\}$;
end
return S;

Suppose the last non-domination level is F_l and solutions of the first $l - 1$ levels have been added to S. The main task of DIR-based selection is to select $N - |S|$ solutions from F_l and add them to S. As it can be seen in Algorithm 4, firstly, the coverage c_j of each solution s^j , estimated by the number of reference vectors a solution covers, is calculated by calling Algorithm 2. The first $|N - |S||$ solutions with the largest coverage values are added to S.

5.2. Experimental settings

To verify the performance of d-NSGA-II on MaOPs, it is compared with its original version NSGA-II [16] and the state-of-art many-objective optimizer, NSGA-III [13] on DTLZ [17] and WFG [21] test suites. To make a fair comparison, simulated

Table 5
The approximation size for all the compared algorithms on MaOPs with different number of objectives.

The number of objectives	3	5	8	10
The approximation size	120	126	156	275

Table 6
Mean and standard deviations of IGD values obtained by NSGA-II, NSGA-III and d-NSGA-II on DTLZ1 to DTLZ4 problems over 30 runs. Wilcoxons rank sum test at a 0.05 significance level is performed to IGD values.

Problem	m	NSGA-II	NSGA-III	d-NSGA-II
DTLZ1	3	$4.9309E-02$ $(2.52E-03)^{-}$	$3.8399E-02$ $(8.70E-03)^{-}$	$3.5176E-02$ $(4.28E-05)$
	5	$1.6002E+01$ $(1.70E+01)^{-}$	$1.3242E-01$ $(2.21E-02)^{-}$	$1.2855E-01$ $(1.94E-04)$
	8	$8.6421E+01$ $(4.56E+01)^{-}$	$3.9603E-01$ $(1.01E-01)^{-}$	$1.8042E-01$ $(2.52E-03)$
	10	$9.1170E+01$ $(4.79E+01)^{-}$	$4.5518E-01$ $(6.93E-02)^{-}$	$1.9582E-01$ $(8.79E-03)$
DTLZ2	3	$6.2893E-02$ $(1.27E-03)^{-}$	$4.6613E-02$ $(8.87E-05)^{\approx}$	$4.6606E-02$ $(4.88E-05)$
	5	$3.2745E-01$ $(2.62E-02)^{-}$	$1.9500E-01$ $(6.07E-05)^{\approx}$	$1.9516E-01$ $(5.24E-05)$
	8	$1.9777E+00$ $(1.12E-01)^{-}$	$6.1565E-01$ $(2.47E-01)^{-}$	$3.9167E-01$ $(5.43E-04)$
	10	$2.1461E+00$ $(1.56E-01)^{-}$	$7.6023E-01$ $(2.10E-01)^{-}$	$4.5666E-01$ $(2.16E-03)$
DTLZ3	3	$6.2035E-02$ $(2.33E-03)^{-}$	$4.6805E-02$ $(2.70E-04)^{\approx}$	$4.6645E-02$ $(8.34E-05)$
	5	$1.2116E+02$ $(5.16E+01)^{-}$	$1.9831E-01$ $(6.56E-03)^{-}$	$1.9674E-01$ $(1.22E-03)$
	8	$4.8112E+02$ $(1.57E+02)^{-}$	$6.7146E-01$ $(2.29E-01)^{+}$	$1.8415E+00$ $(1.16E+00)$
	10	$6.3822E+02$ $(1.83E+02)^{-}$	$8.6548E-01$ $(1.21E-01)^{+}$	$4.8436E+00$ $(3.46E+00)$
DTLZ4	3	$6.1731E-02$ $(2.50E-03)^{-}$	$1.1252E-01$ $(1.71E-01)^{-}$	$4.6599E-02$ $(3.56E-05)$
	5	$2.6674E-01$ $(1.04E-02)^{-}$	$2.0985E-01$ $(8.14E-02)^{-}$	$1.9514E-01$ $(6.38E-05)$
	8	$2.1950E+00$ $(4.39E-02)^{-}$	$3.9359E-01$ $(2.24E-02)^{-}$	$3.9208E-01$ $(1.08E-03)$
	10	$2.3487E+00$ $(3.54E-02)^{-}$	$4.5111E-01$ $(3.61E-03)^{+}$	$4.5967E-01$ $(4.82E-03)$

"+" means the IGD value of the algorithm on this problem is significantly better than that of d-NSGA-II.
"−" means the IGD value of the algorithm on this problem is significantly worse than that of d-NSGA-II.
"≈" means there is no significant difference between the compared results.

binary crossover (SBX) and polynomial mutation are used for all the compared algorithms. The crossover probability p_c is set to 1 and the distribution index η_c is set to 30; the mutation probability p_m is set to $1/l$, where l is the number of decision variables and its distribution index η_m is set to 20 for all the compared algorithms. The approximation size on MaOPs with different number of objectives are given in Table 5. Each test instance is run 30 times and the maximum number of generations is set to 1000. In addition, the reference vectors adopted in d-NSGA-II is the same as the ones used in NSGA-III [13].

Inverted Generational Distance (IGD) [6] is used to evaluate the performance of all the compared algorithms for DTLZ test suite. HV [49] is used for WFG test suite as the true PFs of test problems are unknown[2].

5.3. Comparison between NSGA-II and NSGA-III

The experimental results obtained by NSGA-II and d-NSGA-II on DTLZ1-4, in terms of IGD, are presented in Table 6. It can be observed that d-NSGA-II performs significantly better than NSGA-II on all the test problems. Similarly, d-NSGA-II performs significantly better than NSGA-II on 27 out of 36 WFG problems, as shown in Table 7.

In addition, d-NSGA-II performs significantly better than NSGA-III on 10 out of 16 DTLZ test problems. There are no significant differences on 3 test problems between d-NSGA-II and NSGA-III. For WFG test suite, d-NSGA-II outperforms NSGA-III on 13 test problems; NSGA-III is better on 7 test problems; and there are no significant difference between the two algorithms on 16 test problems.

From Table 7, it can be observed that d-NSGA-II (or NSGA-III) is significantly worse than NSGA-II on 8- and 10-objective WFG2 and all WFG3 instances. The explanation is that WFG2 instances have the discontinuous PFs and WFG3 instances have the degenerate PFs. NSGA-II is more robust to problems with these irregular PFs due to the use of crowding distance estimation for maintaining diversity. On the contrary, the uniformly generated reference vectors are used in d-NSGA-II (or NSGA-III) for maintaining diversity. The potential assumption is that PFs of MOPs are regular; otherwise, a large number of reference vectors may lead to the same Pareto optimal solutions on the boundary of PFs, which causes the waste of many reference vectors.

A possible explanation of causing d-NSGA-II worse than NSGA-III on some instances, is that instead of selecting N solutions with the best (lowest) DIR value, a more greedy method, that selects the first N solutions covering most reference vectors, is used in d-NSGA-II, to avoid high computational burden. By using this greedy strategy, the selection of the solution set with the best diversity in every generation is not guaranteed. To understand the evolving diversity in the three compared algorithms, DIR values in the run with median values during the optimization process for 3-, 5- and 10-objective

[2] The reference points of HV are set as $(3, 5, \ldots, 2m+1)^T$, where m is the number of objectives.

Table 7
Mean and standard deviations of HV values obtained by NSGA-II, NSGA-III and d-NSGA-II on WFG1 to WFG9 problems over 30 runs. Wilcoxon's rank sum test at a 0.05 significance level is performed to HV values.

Problem	m	NSGA-II	NSGA-III	d-NSGA-II
WFG1	3	$7.8943E+01$ $(3.42E+00)^{-}$	$7.9095E+01$ $(2.72E+00)^{-}$	$8.7132E+01$ $(3.59E+00)$
	5	$4.6833E+03$ $(2.79E+02)^{\approx}$	$5.2317E+03$ $(3.65E+02)^{-}$	$5.5116E+03$ $(3.07E+02)$
	8	$1.2866E+07$ $(1.14E+06)^{-}$	$2.2777E+07$ $(1.18E+06)^{+}$	$1.6467E+07$ $(1.58E+06)$
	10	$4.7414E+09$ $(4.17E+08)^{-}$	$1.1155E+10$ $(4.15E+08)^{+}$	$8.4155E+09$ $(1.07E+09)$
WFG2	3	$9.5701E+01$ $(6.50E+00)^{\approx}$	$9.4294E+01$ $(7.64E+00)^{\approx}$	$9.4250E+01$ $(7.53E+00)$
	5	$1.0223E+04$ $(3.18E+01)^{\approx}$	$9.7714E+03$ $(8.23E+02)^{-}$	$9.9542E+03$ $(6.94E+02)$
	8	$3.4136E+07$ $(5.47E+04)^{+}$	$3.1500E+07$ $(3.09E+06)^{\approx}$	$3.2627E+07$ $(2.49E+06)$
	10	$1.3616E+10$ $(4.08E+07)^{+}$	$1.3336E+10$ $(7.80E+08)^{+}$	$1.3224E+10$ $(8.62E+08)$
WFG3	3	$7.5251E+01$ $(1.86E-01)^{+}$	$7.4116E+01$ $(3.91E-01)^{\approx}$	$7.4253E+01$ $(2.87E-01)$
	5	$7.0211E+03$ $(6.82E+01)^{+}$	$6.6939E+03$ $(7.58E+01)^{-}$	$6.6687E+03$ $(9.74E+01)$
	8	$2.2369E+07$ $(5.83E+05)^{+}$	$2.0531E+07$ $(1.05E+06)^{+}$	$1.8652E+07$ $(5.59E+05)$
	10	$9.0532E+09$ $(1.17E+08)^{+}$	$8.3463E+09$ $(6.04E+08)^{+}$	$7.4787E+09$ $(2.19E+08)$
WFG4	3	$7.3745E+01$ $(4.52E-01)^{-}$	$7.6577E+01$ $(1.16E-01)^{\approx}$	$7.6603E+01$ $(1.40E-01)$
	5	$7.1556E+03$ $(1.93E+02)^{-}$	$8.8259E+03$ $(4.22E+01)^{\approx}$	$8.7943E+03$ $(3.98E+01)$
	8	$1.8072E+07$ $(7.57E+05)^{-}$	$3.0686E+07$ $(1.35E+05)^{+}$	$3.0474E+07$ $(2.96E+05)$
	10	$6.8055E+09$ $(2.56E+08)^{-}$	$1.2382E+10$ $(9.89E+07)^{\approx}$	$1.2373E+10$ $(7.55E+07)$
WFG5	3	$7.1093E+01$ $(4.29E-01)^{-}$	$7.3275E+01$ $(3.16E-01)^{-}$	$7.3536E+01$ $(1.85E-01)$
	5	$7.2214E+03$ $(1.45E+02)^{-}$	$8.5604E+03$ $(2.47E+01)^{\approx}$	$8.5638E+03$ $(2.64E+01)$
	8	$1.7629E+07$ $(7.69E+05)^{-}$	$2.9990E+07$ $(1.09E+05)^{\approx}$	$2.9994E+07$ $(8.42E+04)$
	10	$6.7719E+09$ $(2.52E+08)^{-}$	$1.2183E+10$ $(4.57E+07)^{-}$	$1.2215E+10$ $(3.95E+07)$
WFG6	3	$7.1443E+01$ $(4.58E-01)^{-}$	$7.3739E+01$ $(3.29E-01)^{\approx}$	$7.3939E+01$ $(4.36E-01)$
	5	$6.9775E+03$ $(2.63E+02)^{-}$	$8.6045E+03$ $(7.27E+01)^{\approx}$	$8.6009E+03$ $(5.56E+01)$
	8	$1.9022E+07$ $(9.04E+05)^{-}$	$3.0483E+07$ $(2.53E+05)^{\approx}$	$3.0494E+07$ $(2.43E+05)$
	10	$7.3291E+09$ $(3.62E+08)^{-}$	$1.2476E+10$ $(1.19E+08)^{\approx}$	$1.2441E+10$ $(1.10E+08)$
WFG7	3	$7.4403E+01$ $(3.70E-01)^{-}$	$7.6959E+01$ $(3.40E-02)^{-}$	$7.7006E+01$ $(3.34E-02)$
	5	$6.8240E+03$ $(2.56E+02)^{-}$	$9.0015E+03$ $(2.24E+01)^{\approx}$	$9.0020E+03$ $(1.70E+01)$
	8	$1.7241E+07$ $(9.65E+05)^{-}$	$3.1812E+07$ $(8.80E+04)^{\approx}$	$3.1779E+07$ $(1.18E+05)$
	10	$6.9431E+09$ $(2.13E+08)^{-}$	$1.2985E+10$ $(4.57E+07)^{+}$	$1.2948E+10$ $(6.58E+07)$
WFG8	3	$6.7201E+01$ $(2.81E-01)^{-}$	$6.9980E+01$ $(2.63E-01)^{-}$	$7.0550E+01$ $(1.37E-01)$
	5	$6.1418E+03$ $(1.11E+02)^{-}$	$7.9085E+03$ $(3.63E+01)^{-}$	$7.9120E+03$ $(3.31E+01)$
	8	$1.8416E+07$ $(6.02E+05)^{-}$	$2.6083E+07$ $(4.07E+05)^{-}$	$2.7173E+07$ $(6.52E+05)$
	10	$7.4764E+09$ $(2.47E+08)^{-}$	$1.0886E+10$ $(1.09E+08)^{-}$	$1.1464E+10$ $(3.25E+08)$
WFG9	3	$6.8051E+01$ $(1.78E+00)^{-}$	$7.0129E+01$ $(2.33E+00)^{\approx}$	$6.8312E+01$ $(1.44E+00)$
	5	$6.3367E+03$ $(1.71E+02)^{-}$	$7.6851E+03$ $(1.90E+02)^{+}$	$7.6329E+03$ $(1.53E+02)$
	8	$1.5583E+07$ $(1.35E+06)^{-}$	$2.5714E+07$ $(6.89E+05)^{-}$	$2.6120E+07$ $(6.98E+05)$
	10	$6.5287E+09$ $(2.60E+08)^{-}$	$1.0337E+10$ $(2.64E+08)^{-}$	$1.0607E+10$ $(2.57E+08)$

"+" means the HV value of the algorithm on this problem is significantly better than that of d-NSGA-II.
"−" means the HV value of the algorithm on this problem is significantly worse than that of d-NSGA-II.
"≈" means there is no significant difference between the compared algorithms.

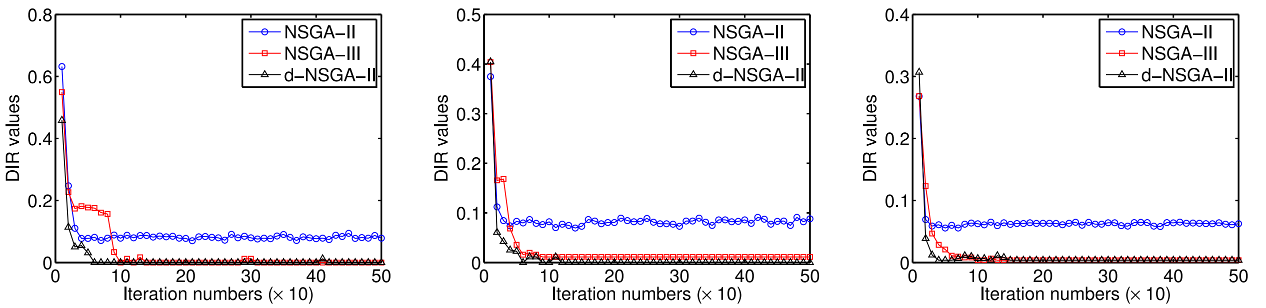

(a) 3-objective DTLZ4 (b) 5-objective DTLZ4 (c) 10-objective DTLZ4

Fig. 12. DIR values of solution sets obtained by NSGA-II, NSGA-III and d-NSGA-II during the optimization process on 3-, 5- and 10-objective DTLZ4.

DTLZ4 and WFG5 are plotted in Figs. 12 and 13. It is clear to see in these figures that d-NSGA-II and NSGA-III maintain much better diversity, in terms of DIR, than NSGA-II. The final DIR values obtained by d-NSGA-II is either better or similar to that obtained by NSGA-III and the decrease of DIR values (better diversity) obtained by d-NSGA-II is much faster than that obtained by NSGA-III, which indicates d-NSGA-II is able to obtain better diversity during the optimization process, due to the use of DIR as an online diversity indicator.

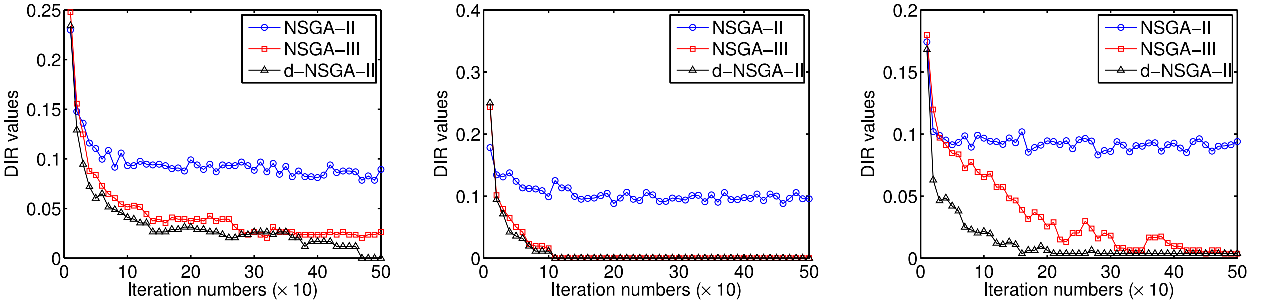

(a) 3-objective WFG5 (b) 5-objective WFG5 (c) 10-objective WFG5

Fig. 13. DIR values of solution sets obtained by NSGA-II, NSGA-III and d-NSGA-II during the optimization process on 3-, 5- and 10-objective WFG5.

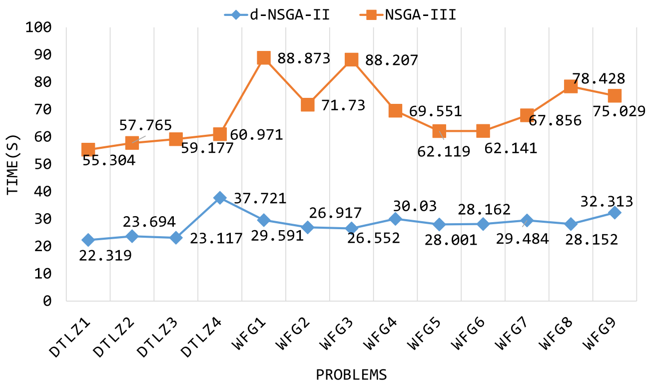

Fig. 14. Computational time used by d-NSGA-II and NSGA-III on a 10-objective optimization problems.

5.4. Computational complexity of d-NSGA-II and NSGA-III

In d-NSGA-II, fast nondominated sorting requires $O(mN^2)$ computations and DIR-based selection requires $O(mMN)$ computations. Therefore, the computational complexity of d-NSGA-II is $max\{O(mMN), O(mN^2)\}$, where m is the number of objectives; N is the approximation size and M is the number of reference vectors ($M = N$ in the experiments). The computational cost of d-NSGA-II is less than that of NSGA-III ($max\left\{O(Nlog^{m-2}N), O(mN^2)\right\}$) [13], when m is a large number for many-objective optimization. The time spent by both algorithms on 10-objective optimization problems is plotted in Fig 14,[3] which shows that d-NSGA-II is more efficient than NSGA-III.

5.5. Applications on real-world optimization problems

In this section, NSGA-II, NSGA-III and d-NSGA-II are implemented and compared on the following two practical engineering optimization problems.

1. Crash-worthiness design of vehicles (CWDV) can be formulated as the structural optimization on the frontal structure of vehicle for crash-worthiness [36]. Thickness of five reinforced members around the frontal structure are chosen as the design variables, while mass of vehicle, deceleration during the full frontal crash and toe board intrusion in the offset-frontal crash are considered as three objectives. More detailed mathematical formulation can be found in [36].
2. Car side-impact problem (CSIP) aims at finding a design that balances between the weight and the safety performance. It is firstly formulated for the minimization of the weight of the car subject to some safety restrictions on safety performance [12]. In [12], it is reformulated as a 9-objective optimization problem by treating some constraints as objectives. More details of the mathematical formulation can be found in [12].

5.5.1. Experimental setups

For CWDV, both the approximation size and the number of reference vectors are set to 120; and the maximum number of iterations is set to 200. For CSIP, both the approximation size and the number of reference vectors are set to 210; and the

[3] The hardware configurations are: AMD A10-5800K APU with Radeon(tm) HD Graphics 3.80 GHz (processor), 6.00GB (5.45GB available, RAM). Two algorithms are all implemented by Java.

Table 8
Mean and standard deviations of IGD or HV values obtained by NSGA-II, NSGA-III and d-NSGA-II over 30 runs on CWDV and CSIP. Wilcoxon's rank sum test at a 0.05 significance level is performed.

Problem	Indicator	NSGA-II	NSGA-III	d-NSGA-II
Crash-worthiness Design	IGD	$3.536E-02\ (7.9E-03)^{\approx}$	$3.603E-02\ (3.7E-03)^{\approx}$	$3.528E-02\ (4.7E-03)$
	HV	$1.029E+00\ (3.1E-03)^{\approx}$	$1.023E+00\ (3.5E-03)^{-}$	$1.027E+00\ (2.5E-03)$
Car Side-Impact Problem	IGD	$1.989E-01\ (7.1E-03)^{-}$	$2.018E-01\ (6.7E-03)^{-}$	$1.800E-01\ (3.4E-03)$
	HV	$2.109E-01\ (1.0E-02)^{-}$	$1.995E-01\ (7.9E-03)^{-}$	$2.454E-01\ (8.5E-03)$

"–" means the HV or IGD value of the algorithm on this problem is significantly worse than that of d-NSGA-II.
"≈" means there is no significant difference between the compared algorithms.

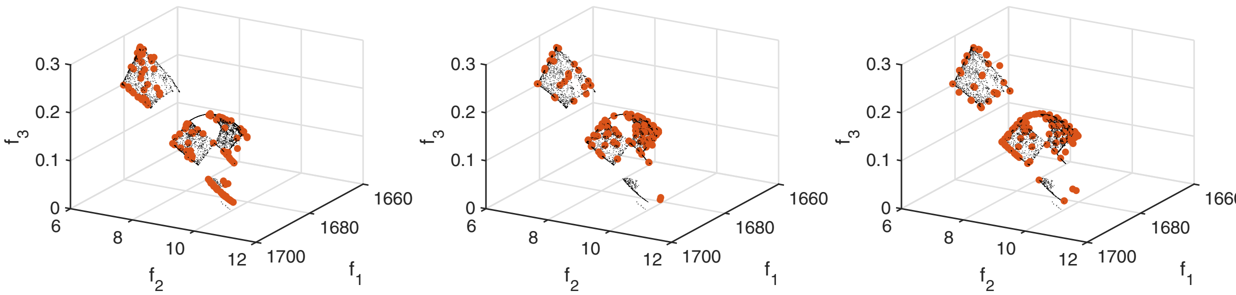

(a) NSGA-II (b) NSGA-III (c) d-NSGA-II

Fig. 15. PF approximations obtained by d-NSGA-II, NSGA-II and NSGA-III in the run with the median IGD values on CWDV.

maximum number of iterations is set to 2000. All the algorithms are run for 30 times for each problem. Other parameters in each algorithm are set the same as that in Section. 5.2.

As the real PFs for both CWDV and CSIP are unknown, a reference PF (denoted as P^*) is constructed by obtaining all the nondominated solutions of all 30 runs obtained by all algorithms for each instance to compute IGD. To calculate HV, the objective values of all the solutions are firstly normalized by their maximal and minimal objective values obtained from P^*; and then, HV values are obtained by using reference point $(1.1, 1.1, \ldots)^T$.

5.5.2. Experimental results

Mean and standard deviations of IGD or HV values obtained by NSGA-II, NSGA-III and d-NSGA-II over 30 runs on CWDV and CSIP are presented in Table 8. For CWDV, d-NSGA-II has the best performance in terms of IGD and NSGA-II has the best performance in terms of HV, without any statistical significance. This indicates the performance of d-NSGA-II and NSGA-II are very similar to each other and both of them perform slightly better than NSGA-III on CWDV. These observations can be further verified in Fig. 15, where PF approximations obtained by three algorithms in the run with the median IGD values are presented.

With respect to CSIP, d-NSGA-II performs significantly better than NSGA-II and NSGA-III in terms of both IGD and HV values. To better visualize the results, PF approximations obtained by d-NSGA-II, NSGA-II and NSGA-III are projected into a bi-objective space for pairwise comparisons, as shown in Fig. 16. It can be observed in Fig. 16(a) that the convergence of d-NSGA-II is better than NSGA-II although the range of solutions obtained by NSGA-II seems larger. In addition, it can be observed in Fig. 16(b) that d-NSGA-II performs better than NSGA-III in terms of both convergence and diversity. All the above experimental results verify the effectiveness of d-NSGA-II, which uses DIR as an online diversity indicator, on real-world optimization problems.

6. Conclusion

In this paper, a unary diversity indicator based on reference vectors (DIR) is proposed based on the following two motivations. 1) A reference vector can be considered as a representative of a subregion in the objective space. The number of reference vectors a solution covers can be used to roughly estimate the coverage of such solution in an approximation. 2) Both the overall coverage and uniformity of an approximation can be measured by the standard deviation of the coverage of all the solutions in an approximation.

Different from other diversity metrics, DIR does not require a substitution of PF and can work well for high dimensional PF approximations. In addition, DIR is a unary metric with relatively low computational cost, which makes it possible to be used as an online indicator for many-objective optimizers. Experimental results show the effectiveness of DIR to measure the diversity of both artificial approximations and the ones obtained by seven MOEAs. Furthermore, DIR is integrated into NSGA-II as an online indicator and the results show that it can significantly enhance the performance of NSGA-II on MaOPs by maintaining satisfactory diversity.

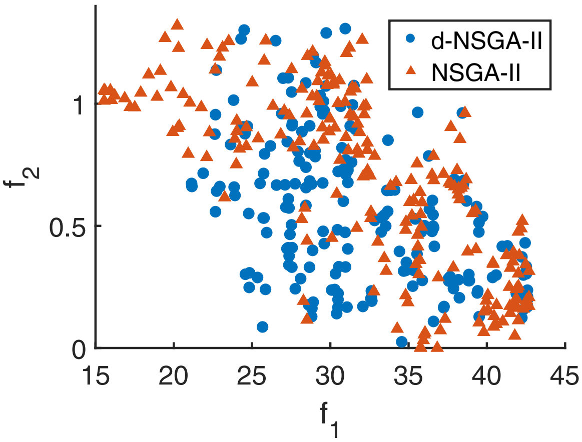

(a) d-NSGA-II vs. NSGA-II

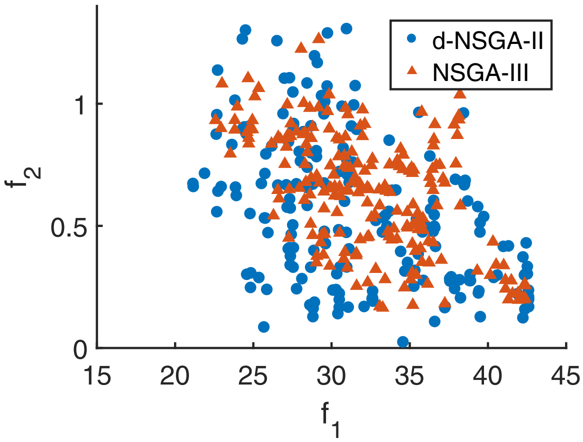

(b) d-NSGA-II vs. NSGA-III

Fig. 16. PF approximations obtained by d-NSGA-II, NSGA-II and NSGA-III in the run with the median IGD values are projected into a bi-objective space for pairwise comparisons on CSIP.

Acknowledgments

This work was supported in part by the National Program on Key Basic Research Project (973 Program) of China under Grant 2014CB744901, Grant 2014CB744903, and Grant 2014CB744904, in part by the National Natural Science Foundation of China under Grant 61300159 and Grant 61473241, in part by the Natural Science Foundation of Jiangsu Province under Grant BK20130808, in part by the China Post-Doctoral Science Foundation under Grant 2015M571751, and in part by the Fundamental Research Funds for the Central Universities of China under Grant NZ2013306 and Grant NS2017070.

References

[1] A. Auger, J. Bader, D. Brockhoff, E. Zitzler, Theory of the hypervolume indicator: optimal-distributions and the choice of the reference point, Found. Genet. Algorithms Acm (2009) 87–102.
[2] F. Aurenhammer, Voronoi diagramsa survey of a fundamental geometric data structure, ACM, 1991.
[3] J. Bader, E. Zitzler, Hype: an algorithm for fast hypervolume-based many-objective optimization, Evol. Comput. 19 (1) (2011) 45–76.
[4] S. Bandyopadhyay, S.K. Pal, B. Aruna, Multiobjective GAs, quantitative indices, and pattern classification, IEEE Trans. Syst. Man Cybern. –Part B 34 (5) (2004) 2088–2099.
[5] N. Beume, B. Naujoks, M. Emmerich, SMS-EMOA: Multiobjective selection based on dominated hypervolume, Eur. J. Oper. Res. 181 (3) (2007) 1653–1669.
[6] P.A. Bosman, D. Thierens, The balance between proximity and diversity in multiobjective evolutionary algorithms, IEEE Trans. Evol. Comput. 7 (2) (2003) 174–188.
[7] X. Cai, Y. Li, Z. Fan, Q. Zhang, An external archive guided multiobjective evolutionary algorithm based on decomposition for combinatorial optimization, IEEE Trans. Evol. Comput. 19 (4) (2015) 508–523.
[8] X. Cai, Z. Mei, Z. Fan, Q. Zhang, A constrained decomposition approach with grids for evolutionary multiobjective optimization, IEEE Trans. Evol. Comput. (2017), doi:10.1109/TEVC.2017.2744674. in press.
[9] C.A. Coello Coello, G.B. Lamont, D.A. Van Veldhuizen, Evolutionary Algorithms for Solving Multi-Objective Problems, Second, Springer, New York, 2007. ISBN 978-0-387-33254-3.
[10] D. Corne, J. Knowles, Techniques for Highly Multiobjective Optimisation: Some Nondominated Points are Better than Others, in: D. Thierens (Ed.), 2007 Genetic and Evolutionary Computation Conference (GECCO'2007), 1, ACM Press, London, UK, 2007, pp. 773–780.
[11] I. Das, J.E. Dennis, Normal-boundary intersection: a new method for generating the pareto surface in nonlinear multicriteria optimization problems, SIAM J. Optim. 8 (3) (1998) 631–657.
[12] K. Deb, S. Gupta, D. Daum, J. Branke, rgen, A.K. Mall, D. Padmanabhan, Reliability-based optimization using evolutionary algorithms, IEEE Trans. Evol. Comput. 13 (5) (2009) 1054–1074.
[13] K. Deb, H. Jain, An evolutionary many-objective optimization algorithm using reference-point-based nondominated sorting approach, part I: solving problems with box constraints, Evol. Comput. IEEE Trans. 18 (4) (2014) 577–601.
[14] K. Deb, S. Jain, Running performance metrics for evolutionary multi-objective optimizations, in: Proceedings of the Fourth Asia-Pacific Conference on Simulated Evolution and Learning (SEAL'02),(Singapore), 2002, pp. 13–20. Proceedings of the Fourth Asia-Pacific Conference on Simulated Evolution and Learning (SEAL'02),(Singapore).
[15] K. Deb, K. Miettinen, Multiobjective Optimization: Interactive and Evolutionary Approaches, 5252, Springer Science & Business Media, 2008.
[16] K. Deb, A. Pratap, S. Agarwal, T. Meyarivan, A fast and elitist multiobjective genetic algorithm: NSGA–II, IEEE Trans. Evol. Comput. 6 (2) (2002) 182–197.
[17] K. Deb, L. Thiele, M. Laumanns, E. Zitzler, Scalable Test Problems for Evolutionary Multiobjective Optimization, in: A. Abraham, L. Jain, R. Goldberg (Eds.), Evolutionary Multiobjective Optimization. Theoretical Advances and Applications, Springer, USA, 2005, pp. 105–145.
[18] P. Fleming, R.C. Purshouse, R.J. Lygoe, Many-Objective Optimization: An Engineering Design Perspective, in: C.A. Coello Coello, A. Hernández Aguirre, E. Zitzler (Eds.), Evolutionary Multi-Criterion Optimization. Third International Conference, EMO 2005, Lecture Notes in Computer Science, 3410, Springer, Guanajuato, México, 2005, pp. 14–32.
[19] S.B. Gee, K.C. Tan, V.A. Shim, N.R. Pal, Online diversity assessment in evolutionary multiobjective optimization: a geometrical perspective, IEEE Trans. Evol. Comput. 19 (4) (2015) 542–559.
[20] Z. He, G.G. Yen, Visualization and performance metric in many-objective optimization, IEEE Trans. Evol. Comput. (2015) 1.
[21] S. Huband, P. Hingston, L. Barone, L. While, A review of multiobjective test problems and a scalable test problem toolkit., Evol. Comput. IEEE Trans. 10 (5) (2006) 477–506.

[22] A. Inselberg, Parallel Coordinates: Visual Multidimensional Geometry and Its Applications, Springer, New York, NY, USA, 2009.
[23] H. Ishibuchi, N. Akedo, Y. Nojima, A many-objective test problem for visually examining diversity maintenance behavior in a decision space, in: Proceedings of the 13th Annual Conference on Genetic and Evolutionary Computation, ACM, 2011, pp. 649–656.
[24] H. Ishibuchi, N. Tsukamoto, Y. Nojima, Evolutionary many-objective optimization: a short review, in: Evolutionary Computation, 2008. CEC 2008. (IEEE World Congress on Computational Intelligence). IEEE Congress on, 2008, pp. 2419–2426.
[25] A.L. Jaimes, C.A.C. Coello, Study of preference relations in many-objective optimization, in: GECCO, 2009, pp. 611–618.
[26] V. Khare, X. Yao, K. Deb, Performance Scaling of Multi-objective Evolutionary Algorithms, in: C.M. Fonseca, P.J. Fleming, E. Zitzler, K. Deb, L. Thiele (Eds.), Evolutionary Multi-Criterion Optimization. Second International Conference, EMO 2003, Lecture Notes in Computer Science, 2632, Springer, Faro, Portugal, 2003, pp. 376–390.
[27] J.D. Knowles, D.W. Corne, The Pareto Archived Evolution Strategy: A New Baseline Algorithm for Multiobjective Optimisation, in: 1999 Congress on Evolutionary Computation, IEEE Service Center, Washington, D.C., 1999, pp. 98–105.
[28] S. Kukkonen, J. Lampinen, GDE3: The third Evolution Step of Generalized Differential Evolution, in: 2005 IEEE Congress on Evolutionary Computation (CEC'2005), 1, IEEE Service Center, Edinburgh, Scotland, 2005, pp. 443–450.
[29] G. Leguizamón, C.C. Coello, Multi-objective ant colony optimization: a taxonomy and review of approaches, Integr. Swarm Intell. Artif. Neural Netw. (2011) 67–94.
[30] H. Li, Q. Zhang, Multiobjective optimization problems with complicated Pareto sets, MOEA/D and NSGA-II, IEEE Trans. Evol. Comput. 13 (2) (2009) 284–302.
[31] K. Li, K. Deb, Q. Zhang, S. Kwong, An evolutionary many-objective optimization algorithm based on dominance and decomposition, Evol. Comput. IEEE Trans. 19 (5) (2015) 694–716.
[32] M. Li, S. Yang, X. Liu, Diversity comparison of pareto front approximations in many-objective optimization, Cybernetics IEEE Trans. 44 (12) (2014) 2568–2584.
[33] M. Li, S. Yang, X. Liu, Shift-based density estimation for pareto-based algorithms in many-objective optimization, Evol. Comput. IEEE Trans. 18 (3) (2014) 348–365.
[34] M. Li, J. Zheng, Spread Assessment for Evolutionary Multi-Objective Optimization, in: M. Ehrgott, C.M. Fonseca, X. Gandibleux, J.-K. Hao, M. Sevaux (Eds.), Evolutionary Multi-Criterion Optimization. 5th International Conference, EMO 2009, Lecture Notes in Computer Science, 5467, Springer, Nantes, France, 2009, pp. 216–230.
[35] M. Li, J. Zheng, G. Xiao, Uniformity Assessment for Evolutionary Multi-Objective Optimization, in: 2008 Congress on Evolutionary Computation (CEC'2008), IEEE Service Center, Hong Kong, 2008, pp. 625–632.
[36] X. Liao, Q. Li, X. Yang, W. Zhang, W. Li, Multi-objective optimization for crash safety design of vehicles using stepwise regression model, Chin. J. Mech. Eng. 35 (6) (2007) 561–569.
[37] K. Miettinen, Nonlinear Multiobjective Optimization, Kluwer Academic Publishers, Boston, 1999.
[38] S. Mostaghim, J. Teich, A new approach on many objective diversity measurement, Pract. Appro. MultiObj. Optim. (2005) 254.
[39] T. Okabe, Y. Jin, B. Sendhoff, A critical survey of performance indices for multi-objective optimisation, in: Evolutionary Computation, 2003. CEC '03. The 2003 Congress on, 2003, pp. 878–885Vol.2.
[40] K.C. Tan, T.H. Lee, E.F. Khor, Evolutionary algorithms for multi-objective optimization: performance assessments and comparisons, Artif. Intell. Rev. 17 (4) (2002) 253–290.
[41] T. Wagner, N. Beume, B. Naujoks, Pareto-, Aggregation-, and Indicator-Based Methods in Many-Objective Optimization, in: S. Obayashi, K. Deb, C. Poloni, T. Hiroyasu, T. Murata (Eds.), Evolutionary Multi-Criterion Optimization, 4th International Conference, EMO 2007, Lecture Notes in Computer Science, 4403, Springer, Matshushima, Japan, 2007, pp. 742–756.
[42] J. Wu, S. Azarm, Metrics for quality assessment of a multiobjective design optimization solution set, Trans. ASME J. Mech. Des. 123 (2001) 18–25.
[43] S. Yang, M. Li, X. Liu, J. Zheng, A grid-based evolutionary algorithm for many-objective optimization, Evol. Comput. IEEE Trans. 17 (5) (2013) 721–736.
[44] G.G. Yen, Z. He, Performance metrics ensemble for multiobjective evolutionary algorithms, IEEE Trans. Evol. Comput.(in press).
[45] Q. Zhang, H. Li, MOEA/D: a multiobjective evolutionary algorithm based on decomposition, IEEE Trans. Evol. Comput. 11 (6) (2007) 712–731.
[46] E. Zitzler, K. Deb, L. Thiele, Comparison of multiobjective evolutionary algorithms: empirical results, Evol. Comput. 8 (2) (2000) 173–195.
[47] E. Zitzler, J. Knowles, L. Thiele, Quality Assessment of Pareto Set Approximations, in: Multiobjective Optimization, 2008, pp. 373–404.
[48] E. Zitzler, S. Künzli, Indicator-based Selection in Multiobjective Search, in: X.Y. et al. (Ed.), Parallel Problem Solving from Nature-PPSN VIII, Lecture Notes in Computer Science, 3242, Springer-Verlag, Birmingham, UK, 2004, pp. 832–842.
[49] E. Zitzler, L. Thiele, Multiobjective evolutionary algorithms: a comparative case study and the strength pareto approach, IEEE Trans. Evol. Comput. 3 (4) (1999) 257–271.
[50] E. Zitzler, L. Thiele, J. Bader, On Set-Based Multiobjective Optimization, Technical Report 300, Computer Engineering and Networks Laboratory, ETH Zurich, 2008.